Remarkable Ability of Horse Spleen Apoferritin To Demetallate Hemin and To Metallate Protoporphyrin IX as a Function of pH

Robert R. Crichton,*,‡ Jose-Antonio Soruco,‡ Francine Roland,‡ Marie-Anges Michaux,§ Bernard Gallois,§ Gilles Précigoux,§ Jean-Pierre Mahy,|| and Daniel Mansuy||

Unité de Biochimie, Université Catholique de Louvain, place Louis Pasteur 1, B-1348 Louvain-la-Neuve, Belgium, Unité de Biophysique Structurale, UPRESA 5471, Université de Bordeaux I, 33405 Talence Cedex, France, and Laboratoire de Chimie et Biochimie Pharmacologiques et Toxicologiques, URA 400 CNRS, Université René Descartes, 45 rue des Saints Pères, 75270 Paris Cedex, France

Received April 21, 1997; Revised Manuscript Received July 24, 1997⊗

ABSTRACT: In previous studies it has been shown that reaction of crystalline horse spleen apoferritin with hemin leads to a protoporphyrin IX−apoferritin complex [Précigoux et al. (1994) *Acta Crystallogr. D50*, 739−743]. We show here the following. (i) Hemin binds to two classes of sites in horse spleen apoferritin at pH 8, each with a binding stoichiometry of 0.5 hemin/subunit; protoporphyrin IX also binds to horse spleen apoferritin with an apparent binding stoichiometry of 1 molecule of protoporphyrin IX/subunit. (ii) When Fe(III)-protoporphyrin IX binds to apoferritin, there is a pH-dependent loss of the metal ion, extremely slow at alkaline pH values (half-time of weeks) and much more rapid at acidic pH values (half-time of seconds below pH 5.0); maximum rates of demetallation are found at pH 4.0, and at lower pH values they decrease. (iii) Chemical modification of 11 carboxyl groups/subunit in horse spleen apoferritin does not affect hemin binding at alkaline pH values; however, it prevents hemin demetallation at acidic pH values. (iv) Hemin that has been demetallated at acidic pH values can be remetallated by increasing the pH; the rate of remetallation is greater at more alkaline pH values. (v) When around 20 atoms of iron/molecule are incorporated into horse spleen apoferritin and protoporphyrin IX is then bound, iron can subsequently be transferred to the porphyrin at pH 8.0. A mechanism is proposed to explain demetallation of heme, involving attack on the tetrapyrrole nitrogens of the protoporphyrin IX-Fe by protons derived from protein carboxylic acid groups and subsequent complexation of the iron by the corresponding carboxylates and binding of protoporphyrin IX to a preformed pocket in the inner surface of the apoferritin protein shell. The cluster of carboxylates involved is situated at the entrance to the pocket in which the protoporphyrin IX molecule is bound and has been previously identified as the site of iron incorporation into L-chain apoferritins. This appears to be the first example of iron removal and incorporation into porphyrins under relatively mild physiological conditions.

Ferritins are a family of proteins that are widely distributed in nature (*1*). They are characterized by a 24 subunit polypeptide shell with the approximate symmetry of a rhombic dodecahedron (point group 432), which encloses a roughly spherical cavity of around 7−9 nm diameter, within which an iron core of variable content and composition is deposited. In mammals, plants, and probably in some invertebrate species, ferritin appears to serve as a soluble, bioavailable, and nontoxic form of iron, in which excess iron can be stored and from which iron can be mobilized when required for cellular requirements. In contrast, although ferritin is found in many microorganisms, from *Escherichia coli* to yeast, it is not at all clear whether it is involved in iron storage. *E. coli* appears to regulate its iron requirements at the level of iron uptake, such that it is hard to see what role iron storage could play in normal iron homeostasis (*2*). When *Saccharomyces cerevisiae* is grown in iron-rich medium, it stores the iron in polyphosphate-rich acidic granules, not in yeast ferritin (*3*), again underlining the unlikely role of this particular ferritin in an iron storage function.

One other feature that clearly distinguishes most bacterial ferritins from eukaryotic ferritins is the presence of heme in the former, usually in a stoichiometry of 1 heme/2 subunits (*4*). The X-ray structure of *E. coli* bacterioferritin has shown that the heme is bound in a pocket within the protein shell formed by the interface between a pair of symmetry-related subunits (*5*). The axial ligands of the heme are the sulfurs of two equivalent methionyl residues from the symmetry-related subunits (*5*−*7*). Although spectroscopic studies have shown that the best-characterized mammalian ferritin, horse spleen ferritin, can bind heme (*8*−*10*), a crystallographic study of single crystals prepared from a mixture containing heme or Sn-protoporphyrin IX showed that the heme-binding sites are occupied by protoporphyrin IX, free of the metal, rather than the original metalloporphyrin (*11*, *12*). The maximum ligand stoichiometry in the crystal state appears to be 12 protoporphyrins/molecule of apoferritin, and the well-defined cleft in the inner side of the protein shell in which the porphyrin is bound corresponds to the heme-binding site in bacterioferritin.

* To whom correspondence should be addressed.
‡ Unité de Biochimie, Université Catholique de Louvain.
§ Unité de Biophysique Structurale.
|| Laboratoire de Chimie et Biochimie Pharmacologiques et Toxicologiques.
⊗ Abstract published in *Advance ACS Abstracts,* November 1, 1997.

S0006-2960(97)00914-8 CCC: $14.00

Table 1: λ_{max} Corresponding to the Soret Band in the UV−Visible Spectra of Protoportphyrin IX and Heme and Their Complexes with BSA and Apoferritin at pH 5.5 and 8

complex	λ_{max} (nm) at pH 5.5	λ_{max} (nm) at pH 8
PPIXFe[a]	411	386
apoferritin−PPIXFe[b]	*c*	410−414
BSA−PPIXFe[b]	393	390
PPIX[a]	361, 415	383, 414
apoferritin−PPIX[b]	368	375

[a] Absolute UV−visible spectra in 0.1 M phosphate buffer, pH 8, or 0.1 M acetate buffer, pH 5.5. [b] Differential UV−visible spectra in the same buffers; the sample cuvette contained 2.5 μM apoferritin− or BSA−PPIXFe or −PPIX and the reference cuvette contained 2.5 μM PPIXFe. [c] No value is given since the spectrum observed a few minutes after adding PPIX-Fe to the apoferritin solution at this pH corresponds to that of PPIX alone with apoferritin.

This paper reports a spectral study of the interaction between heme and horse spleen apoferritin as a function of pH. It shows not only that this protein removes iron from heme at acidic pH but also that it can reincorporate iron into protoporphyrin IX at more basic pH. Evidence is presented from chemical modification that carboxyl groups are involved in heme demetallation. We conclude that horse spleen apoferritin, and perhaps mammalian ferritins in general, have preserved their heme-binding site but have acquired the capacity to demetallate the porphyrin. A mechanism for heme demetallation is proposed.

MATERIALS AND METHODS

Horse spleen apoferritin, ferritin, bovine serum albumin, and the buffers MOPS,[1] MES, and HEPES were from Sigma (St. Louis, MO). Chelex 100 was from Bio-Rad (Nazareth, Belgium). PPIX and PPIX-Fe were from Porphyrin Products (Logan, UT). Apoferritin was prepared from ferritin using 0.5% thioglycolate, adjusted to pH 5.5 as in ref *13*.

Binding studies of Fe(III)-protoporphyrin IX and of protoporphyrin IX were carried out by incubating the apoferritin at a concentration of 1 mg/mL in a suitable buffer with the porphyrin derivative at an appropriate concentration—typically from 0.1 to 1.2 equiv of porphyrin/apoferritin subunit (corresponding to 1−30 porphyrin molecules/apoferritin)—and measuring their spectra between 250 and 650 nm against the same concentration of porphyrin in the same buffer. Buffers used were 0.1 M sodium phosphate (pH 8.0−5.0) and sodium acetate (pH 5.0−5.5). Spectra were recorded with a Shimadzu UV 160 spectrophotometer (Shimadzu, Berchem, Belgium) or with a Uvikon 860 (Kontron Instruments, France). The absorption maxima corresponding to the Soret band in the UV−visible spectra of protoporphyrin IX (PPIX) and hemin (PPIX-Fe) and of their complexes with bovine serum albumin (BSA) and apoferritin at pH 5.5 and 8.0 are presented in Table 1. No value is given for hemin with apoferritin at pH 5.5 since the spectrum observed a few minutes after adding the PPIX-Fe to the apoferritin solution corresponded to that of PPIX alone with apoferritin (i.e., 368 nm).

[1] Abbreviations: PPIX, protoporphyrin IX; PPIX-Fe, hemin (Fe^{3+}-protoporphyrin IX); EDC, 1-ethyl-3-[3-(dimethylamino)propyl]carbodiimide; MOPS, 3-morpholinopropanesulfonic acid; MES, 2-morpholinoethanesulfonic acid; HEPES, 4-(2-hydroxyethyl)piperazine-1-ethanesulfonic acid; BSA, bovine serum albumin; BFr, bacterioferritin; rL apoferritin, recombinant L-chain apoferritin.

Iron uptake into apoferritins was measured using freshly prepared solutions of $(NH_4)Fe(SO_4)_2 \cdot 6H_2O$ in 0.1 M Hepes (pH 7.0−8.0), MOPS (pH 6.5−7.9), or MES (pH 5.8−6.5) as described in ref *14*.

Glycineamide and taurine modifications were carried out by the method of ref *15*. To the protein solution (10 mL at a concentration of 1.5 mg/mL) at room temperature, was added the glycineamide or taurine in solid form; the pH adjusted to 4.75 and the EDC was added, also in solid form. Over 48 h the addition of nucleophile and of EDC was continued at pH 4.75 to attain a final concentration of 1 M for glycineamide, 0.5 M for taurine, and 0.1 M for EDC. The solution was dialyzed extensively for several days to remove excess reagents, and samples (0.1 mg of protein) were taken for amino acid analysis, which was carried out in triplicate after 16 h of hydrolysis in 6 N HCl at 110 °C using a Locarte amino acid analyzer (Locarte Co., London, U.K.). The number of residues modified was determined for glycineamide by the increase in the number of glycine residues/subunit compared to unmodified horse spleen apoferritin using alanine as reference, and for taurine by including an authentic sample of taurine in the standard amino acid mixture used for calibration. In order to eliminate interference with the taurine determination, 3% methanol was added to the pH 3.25 sodium citrate buffer, and no thiodiglycol was included in either the second or the third buffer (pH 4.25 sodium citrate and pH 9.7 sodium borate, respectively).

RESULTS

The absorption maxima observed for both hemin and protoporphyrin IX bound to apoferritin at pH 8.0 and 5.5 (Table 1) indicate clearly that when difference spectra are measured against porphyrin as blank, there is no difficulty in distinguishing the metallated from the demetallated form of the porphyrin. When horse spleen apoferritin (1 mg/mL) in 0.1 M sodium phosphate buffer, pH 8.0, was incubated with incremental concentrations of hemin (from 1 up to 30 molecules of hemin/molecule of apoferritin) for 15 min and the spectra were registered against a reference solution containing the same final concentration of hemin, spectra similar to those shown in Figure 1a were obtained. The stoichiometry of binding can be estimated from the graphical representation (Figure 1b) of the absorbance at 410 nm against the number of equivalents of hemin/molecule of apoferritin. There appear to be two plateaus for hemin binding corresponding to 12 and 24 equiv/molecule of apoferritin. This is in contrast to the binding of protoporphyrin IX under the same conditions, which shows an absorbance maximum at 370 nm and a binding stoichiometry of about 20 equiv/apoferritin molecule (Figure 2). The spectra observed after binding of protoporphyrin IX to apoferritin did not change even after several weeks. However, in the case of hemin binding, when the spectra were registered after several weeks (Figure 1c) a second absorption maximum was seen at around 375 nm, accompanied by a decrease in the absorbance at 410 nm. From the data presented above it was reasonable to assume that this second peak corresponds to the demetallated form of the heme. Accordingly, when horse spleen apoferritin (1 mg/mL) in 0.1 M sodium phosphate buffer, pH 7.6, to which 4 hemin/apoferritin have been added is adjusted to pH 6.2, the maximum at 410 nm corresponding to the PPIX-Fe de-

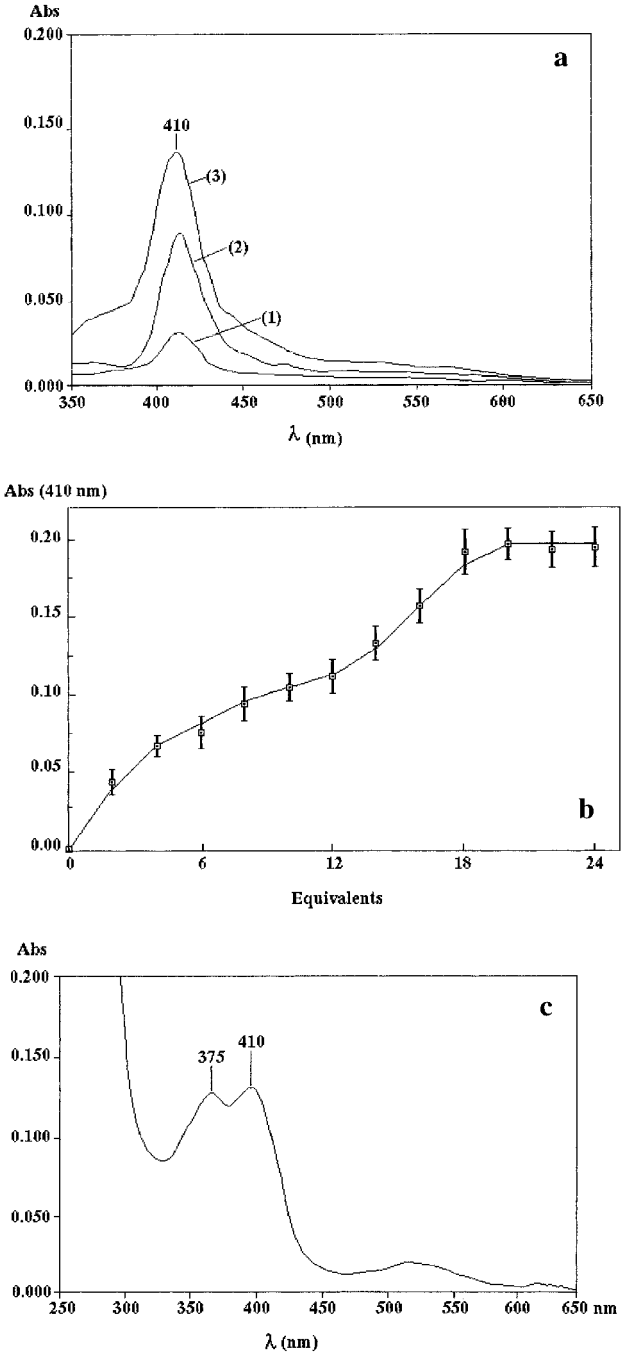

FIGURE 1: (a) Binding of hemin to horse spleen apoferritin (1 mg/mL) in 0.1 M sodium phosphate buffer, pH 8.0. Hemin was added at a respective stoichiometry of (1) 2 hemin, (2) 8 hemin, and (3) 16 hemin per apoferritin molecule and the spectra were measured against a reference cuvette containing the same concentration of hemin 15 min after addition. (b) The increase in absorbance at 410 nm after 15 min is plotted as a function of the amount of hemin added per apoferritin molecule (as in panel a at a protein concentration of 1 mg/mL), represented as equivalents of hemin bound. (c) Binding of hemin in 0.1 M sodium phosphate buffer, pH 8.0, at a concentration of 4 hemin/apoferritin molecule: the spectral trace was recorded after 23 days at room temperature. The second absorption maximum observed at 375 nm corresponds to protoporphyrin IX.

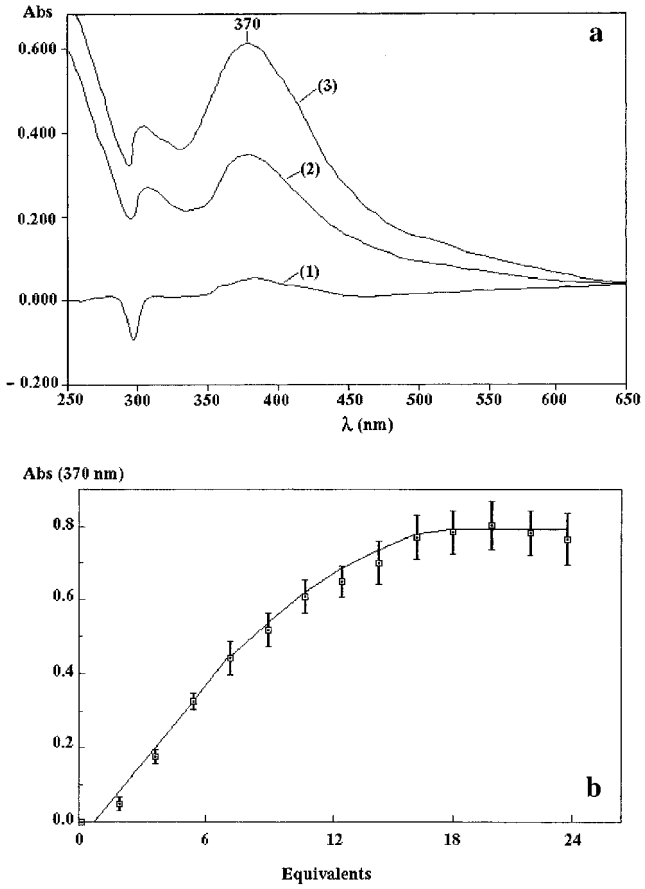

FIGURE 2: (a) Binding of PPIX to horse spleen apoferritin (1 mg/mL) in 0.1 M sodium phosphate buffer, pH 8.0. PPIX was added at a respective stoichiometry of (1) 2 PPIX, (2) 8 PPIX, and (3) 12 PPIX per apoferritin molecule, and the spectra were measured 15 min after addition. (b) The increase in absorbance at 370 nm is plotted as a function of the amount of PPIX added per apoferritin molecule (as in panel a at a protein concentration of 1 mg/mL), represented as equivalents of PPIX bound.

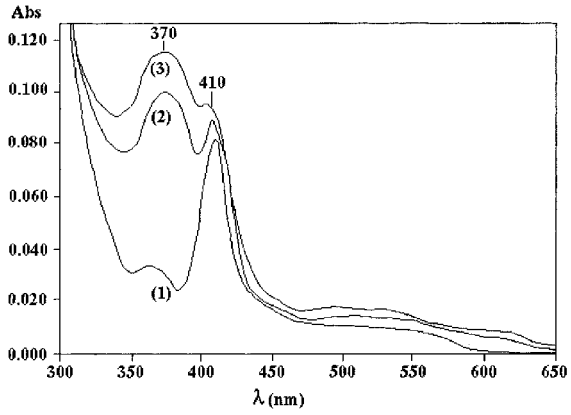

FIGURE 3: Demetallation of hemin by horse spleen apoferritin. Hemin (4 equiv/apoferritin molecule) was added to horse spleen apoferritin (1 mg/mL) in 0.1 M sodium phosphate buffer, pH 7.6. The pH was then adjusted to 6.2, and spectra recorded after (1) 1 min, (2) 11 min, and (3) 2 h 37 min show the increase in the peak at 370 nm and the corresponding assimilation of the 410 nm peak into the PPIX spectrum.

creases, while the metal-free PPIX maximum at 370−375 nm grows with time (Figure 3). The rate of demetallation as a function of pH is presented in Figure 4. Analysis of Figure 4 indicates an initial phase between pH 6.5 and 4.0, which is characterized by a gradual increase in rate, and an inflection around pH 4.5. This would correspond to the p*K* of protein carboxylates. Below pH 4, the rate of demetallation decreases. We have not carried out measurements below pH 3.0, since apoferritin is known to dissociate into subunits at lower pH values (*16*). At pH 8 the half-time for demetallation is several weeks, whereas at pH 5.0 it is on the order of minutes. It is noteworthy that similar experi-

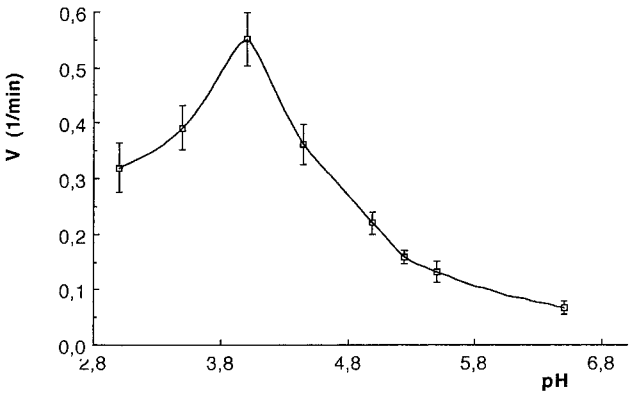

FIGURE 4: pH dependence of demetallation of hemin by apoferritin. The rate of demetallation (A_{370}/min) was measured in 0.1 M sodium phosphate buffers at pH values between 6.5 and 3.0. The rate was estimated by the tangent at the origin of the traces representing A_{370} versus time.

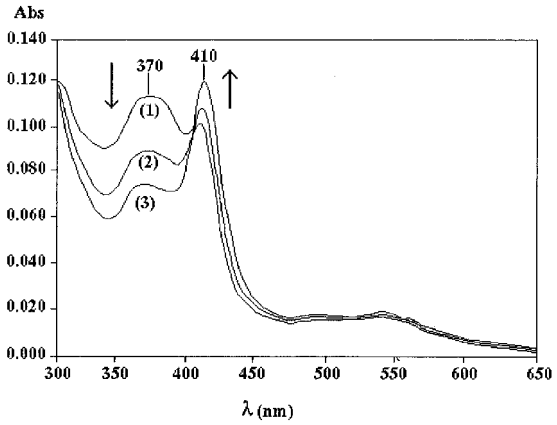

FIGURE 5: Remetallation of PPIX. Apoferritin (1 mg/mL) that had been incubated with 4 hemin/molecule in 0.1 M sodium phosphate buffer, pH 6.2, for 2 h 37 min was adjusted to (1) pH 6.4, (2) pH 6.8, and (3) pH 7.0. Spectra were recorded after 5 min.

ments performed on hemin and BSA did not show any change in the spectrum of the BSA−hemin complex even at pH 5.5.

When apoferritin in which 11 carboxyl groups had been modified by glycineamide in the presence of a water-soluble carbodiimide was incubated with hemin (4 hemin/apoferritin) in 0.1 M phosphate buffer at pH 8.0 (data not shown), as expected, no change was observed in the spectrum, with the λ_{max} remaining constant at 413 nm after 10 min. When the same chemically modified apoferritin was incubated with hemin (same concentration) in 0.1 M phosphate buffer at pH 6.5, no change was observed in either the intensity or the λ_{max}, which remained constant at 414 nm after a 27 min incubation (data not shown). Similar results were obtained at lower pH values and during longer periods of incubation at pH 6.5.

Not only can hemin be demetallated by apoferritin, the iron can also be reincorporated by increasing the pH. Figure 5 shows the spectrum of the sample of hemin that has been demetallated at pH 6.2 and then readjusted to more alkaline pH values. When the pH increases, the maximum at 410 nm increases while that at 370 nm decreases, indicating that the iron is presumably not very far from the porphyrin.

In order to establish whether apoferritin in which iron had been accumulated could transfer this iron to PPIX, apoferritin at a concentration of 1 mg/mL was incubated in HEPES buffer, 0.1 M, pH 7.0, for 24 h with a quantity of ferrous ammonium sulfate corresponding to 20 atoms of Fe/apoferritin molecule. The apoferritin preparation was then passed through a small column of Chelex 100, to remove any unbound iron. PPIX (2 molecules of PPIX/molecule of apoferritin) was added to apoferritin and to apoferritin that had been incubated with iron, both in sodium phosphate buffer, pH 8.0, and the spectra were measured after 10 min (data not shown). The PPIX maximum at 377.5 nm of the iron-free apoferritin shifts after 10 min in the iron-containing apoferritin to a λ_{max} of 406.5 nm, more characteristic of PPIXFe bound to apoferritin.

DISCUSSION

The binding stoichiometry observed for hemin indicates two binding sites, one of which is occupied at lower hemin concentrations, each corresponding to 1 hemin/2 subunits. In contrast, PPIX seems to bind with a stoichiometry of about 1 molecule/subunit. Crystallographic studies reveal one binding site for protoporphyrin IX, which has been demetallated, located on a 2-fold symmetry axis passing through the dimer some 10 Å inside the outer surface of the protein shell with a maximum ligand stoichiometry of 12 porphyrins/molecule. Why the second site is not seen in the X-ray structure could have several explanations. One of these could arise from a porphyrin unit with a disordered orientation, binding close to but not on a 2-fold axis such that binding to one subunit prevented binding to the adjacent subunit in the 2-fold linked dimer, the ligand stoichiometry would be only 0.5 (i.e., 12 porphyrins/molecule). Such a low value, associated with local disorder, would explain why the porphyrin would not be observed by X-ray crystallography. This second site could be located either on the inside or on the outside of the protein shell. Alternatively, several binding sites might be considered, such as, for instance, different hydrophilic lateral amino acid side chains, protruding from the inside of the protein shell, and susceptible to establishing hydrogen bonds with the porphyrin's propionate groups. In such a configuration, in order to satisfy the stoichiometry of 0.5, each binding site has to be statistically occupied by a porphyrin molecule that is still in a disordered orientation.

One of the reasons for undertaking the present study was to cast more light on the interesting findings that when horse spleen apoferritin was crystallized with Fe- or Sn-protoporphyrin IX, the heme-binding sites in the crystals are occupied by protoporphyrin IX that is free of metal, rather than the original metalloporphyrin (*11*). More recent studies with Pt-hematoporphyrin IX and Sn-protoporphyrin IX have shown that only protoporphyrin IX significantly interacts with the protein, whereas hematoporphyrin does not, although both metalloporphyrins are demetallated (*12*). In the present solution studies we have shown that demetallation can be followed by the disappearance of the absorption maximum at around 410 nm that was found for the hemin−apoferritin complex, and its progressive replacement by a new maximum at around 360−370 nm that is characteristic of PPIX bound to apoferritin. Analysis of the pH dependence of the demetallation (Figure 4) shows it to be associated with one or more residues with a p*K* around 4.5—most probably carboxylates. It has been noted before (*12*, *17*) that the site in which the porphyrin is found is close to the three residues, Glu 53, Glu 56, and Glu 57, that have been identified from chemical modification, kinetic, and mass spectroscopic

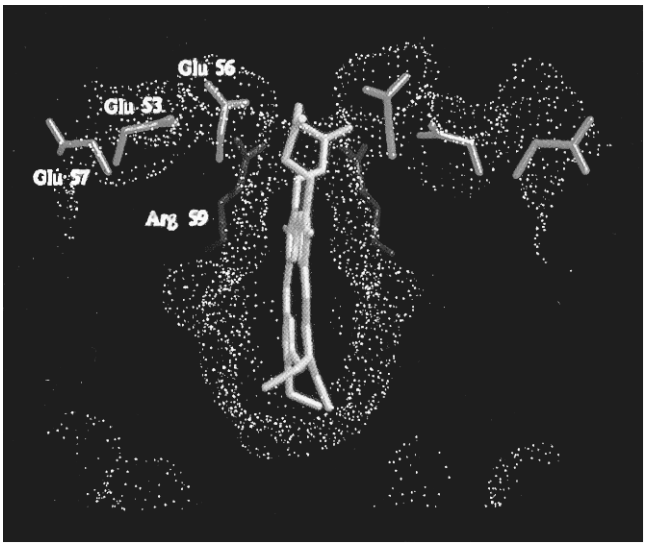

FIGURE 6: Protoporphyrin binding pocket, showing the proximity of the cluster of Glus and Arg 59.

studies as being involved in catalysis of iron uptake by L-chain apoferritins (*14*). The catalytically active carboxylates of the predominantly L-chain horse spleen apoferritin are close to the external propionate groups of the protoporphyrin IX molecule in the predominantly hydrophilic outer part of the porphyrin binding pocket. As we show in Figure 6, Glu 56 is within hydrogen-bonding distance of the propionate groups of the porphyrin, and Glu 53 is within hydrogen-bonding distance of Glu 56 (not shown). The third residue, Glu 57, is also close by, as is Glu 60. From the symmetry-related subunit, Arg 59 is also within salt bridge-forming distance of each of the propionate groups. While we have no proof that any or all of these residues participate directly in demetallation of the porphyrin, they are all located at the narrow entry to the porphyrin-binding pocket. Further, the ease with which remetallation can be achieved by raising the pH (and increasing the population of deprotonated carboxylates) leads us to the conclusion that the iron cannot be located very far away from the protoporphyrin IX binding site. As described above, results from the chemical modification of these catalytic carboxylates indicate that their modification blocks the demetallation reaction. If the carboxyl groups in question are directly involved in demetallation, the mechanism by which they catalyze the ejection of the iron from the Fe-protoporphyrin IX remains to be established. We can, however, postulate a plausible mechanism (Figure 7), assuming that heme demetallation is favored by several factors: (i) the proximity to the heme tetrapyrrole nitrogens of a source of protons—this could be either Arg 59 or some of the carboxylic acid functions of the cluster of glutamates; (ii) complexation of the iron atom by appropriate side-chain residues in proximity to the porphyrin could help to pull the equilibrium in favor of demetallation (molecular vacuum cleaner effect); and (iii) nesting of the protoporphyrin in the preformed pocket.

Obviously, the presence of potential proton donors in the proximity of heme could assist in the protonation of the tetrapyrrole nitrogen ring ligands, enabling the iron to be released from its pentacoordinate (or hexacoordinate) geometry. The candidates are Arg 59 and the cluster of Glus—53, 56, 57, and 60. The pH dependency of heme demetallation would seem to plead in favor of the Glus, which become more likely to be protonated as the pH becomes more acidic (Figure 4) rather than Arg 59, which would remain protonated in the pH range 8−5. The decrease in the rate of demetallation at pH values below 4 (Figure 4) could be interpreted as reflecting the fact that protonation of the Glu cluster, while still supplying protons for attack of the heme, renders the Glu residues unable to chelate the iron ion, and hence abolishes the molecular vacuum cleaner effect (Figure 7). The involvement of the Glu residues 53, 56, and 57 is heavily supported by the abolishment of demetallation in apoferritin in which these Glu residues have been modified with glycineamide. That reduction of Fe^{3+} to Fe^{2+} is involved seems unlikely since there are no potential electron donors among the adjacent side chains and the potential iron binding ligands are carboxylates, which are excellent ligands of Fe^{3+} rather than of Fe^{2+}. The potential roles of iron complexation and of the nesting of the protoporphyrin IX as factors that could potentially pull the demetallation are now considered. If the cluster of carboxylates functions as an iron binding site, this could enhance the potential for demetallation. That this is an iron binding site in L-chain apoferritins has been established recently (*14*). Moreover, in the X-ray structure of recombinant L-chain horse apoferritin, electron density is found close to this site. This electron density, initially fitted with three disordered water molecules, (*17*), has been clearly identified using anomalous Fourier difference map calculation as a privileged site for different metal ions, such as cadmium or iron (T. Granier, G. Comberton, B. Gallois, B. Langlois d'Estaintot, A. Dautant, R. R. Crichton, and G. Précigoux, unpublished data). We may tentatively conclude that there are good reasons to believe that iron is indeed bound close to the pocket in which PPIX is found by X-ray crystallography. This would also explain remetallation of the porphyrin when

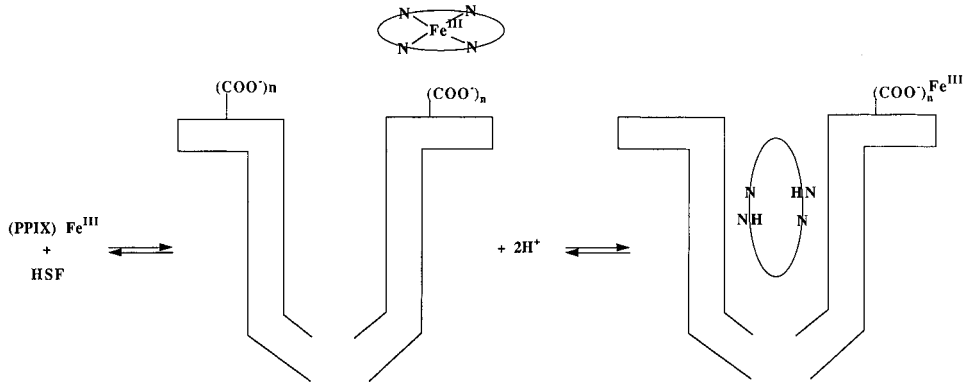

FIGURE 7: Mechanism for demetallation/remetallation in horse spleen apoferritin. The porphyrin ring is represented by an oval.

the pH is increased in the presence of apoferritin to which iron has first been bound.

The nesting effect resides in the observation that X-ray data indicates that if hemin were to bind in the cavity in which protoporphyrin is bound, there would be no place for axial ligands (*12*). This suggests, although in view of the plasticity of the apoferritin molecule does not prove, that protoporphyrin IX would bind preferentially to the site that is found from X-ray crystallographic studies (*11*, *12*), thus explaining why hemin binding, under conditions that do not favor demetallation (on account of the short times used for the studies) give quite different results from protoporphyrin IX binding. When protoporphyrin IX is bound to horse spleen apoferritin under crystallization conditions, it is found in the same site that is found with hemin under the same conditions (*18*). This underlines the precautions that must be undertaken when comparing crystallographic data with solution studies (the time scales are typically several orders of magnitude longer for the former than the latter). One possible explanation could be that the porphyrin binding pocket opens to a greater extent at alkaline than at acidic pH values. We can conclude that, in hemin demetallation in horse spleen apoferritin, it is not unlikely that the effects of protonation of the ring nitrogens, the chelation potential of the carboxylates, and the nesting effect of the protoporphyrin are all involved.

In bacterioferritin (BFr) there is a total transformation of the residues which form the exterior of the heme-binding pocket: Glu 53 has become His, Glu 56 is now Ile, Glu 57 has become Asp, and Glu 60 is now Lys. Finally, Arg 59 is replaced by Met and has changed its configuration. Unlike Arg 59 in rL chain horse apoferritin, which points out of the pocket to form salt bridges with the propionic side chains of the porphyrin, Met 59 in BFr occupies the two axial liganding positions to the heme iron (*5*).

When the structure of BFr is compared to horse spleen apoferritin complexed with PPIX, it is apparent that in BFr the pocket is more open, that there are organized water molecules in the bottom of the pocket, and that the porphyrin is held out of the pocket by a few angstroms compared to the mammalian protein (Figure 8). We could conclude that iron remains bound within the protoporphyrin nucleus on account of the lack of protonation possibilities at the external surface of the pocket, the presence of potential iron binding ligands (Met 59), and the opening of the porphyrin binding pocket to allow binding of heme rather than of protoporphyrin IX.

When we consider the situation in H-chain apoferritins, we have the following situation: Glu 53 becomes His, as does Glu 56, and Glu 57 remains unchanged, as do Glu 60 and Arg 59. However, Arg 59 forms a hydrogen bond with Ser 55, and His 56 swings over to effectively block the porphyrin binding domain. This sugggests that H-chain apoferritins would not supply the nesting environment found in L-chain apoferritins nor the totality of the carboxylate cluster found around Glu 53, Glu 56, Glu 57, and Glu 60.

In conclusion, the present study with horse spleen apoferritin, a predominantly L-chain rich ferritin, appears to be the first example of iron removal from, and incorporation into, porphyrins under relatively mild physiological conditions.

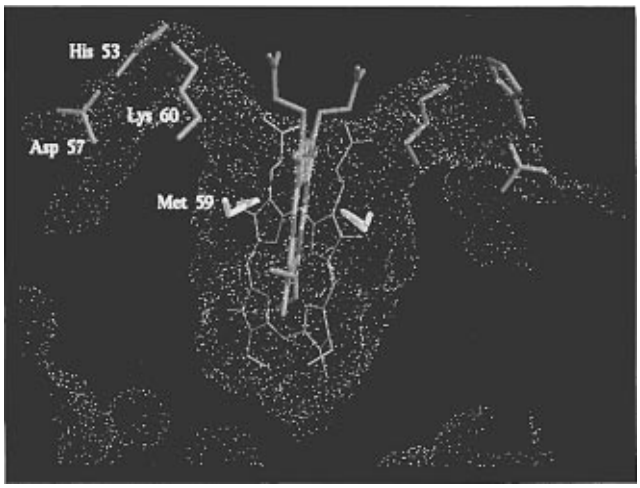

FIGURE 8: Comparison of the porphyrin binding sites in BFr and rL horse apoferritin.

REFERENCES

1. Crichton, R. R., & Ward, R. J. (1992) *Biochemistry 31*, 11255−11264.
2. Braun, V. (1995) *FEMS Microbiol. Rev. 16*, 295−307.
3. Raguzzi, F., Lesuisse, E., & Crichton, R. R. (1988) *FEBS Lett. 231*, 253−258.
4. Briat, J.-F. (1992) *J. Gen. Microbiol. 138*, 2475−2483.
5. Frolow, F., Kalb (Gilboa) A. J., & Yariv, J. (1994) *Nat. Struct. Biol. 1*, 453−460.
6. Cheesman, M. R., Thomson, A. J., Greenwood, C., Moore, G. R., & Kadir, F. H. A. (1990) *Nature 346*, 771−773.
7. Moore, G. R., Cheesman, M. R., Kadir, F. H. A., Thomson, A. J., Yewdall, S. J., & Harrison, P. M. (1990) *Biochem. J. 287*, 457−460.
8. Kadir, F. H. A., & Moore, G. R. (1990) *FEBS Lett. 276*, 81−84.
9. Moore, G. R., Kadir, F. H. A., & Al-Massad, F. K. (1992) *J. Inorg. Biochem. 47*, 175−181.
10. Kadir, F. H. A., Al-Massad, F. K., & Moore, G. R. (1992) *Biochem. J. 282*, 867−880.
11. Précigoux, G., Yariv, J., Gallois, B., Dautant, A., Courseille, C., & Langlois d'Estaintot, B. (1994) *Acta Crystallogr. D50*, 739−743.
12. Michaux, M.-A., Dautant, A., Gallois, B., Granier, T., Langlois d'Estaintot, B. & Précigoux, G. (1996) *Proteins: Struct., Funct., Genet. 24*, 314−321.
13. Bryce, C. F. A., & Crichton, R. R. (1973) *Biochem. J. 131*, 301−309.
14. Crichton, R. R., Herbas, A., Chavez-Alba, O., & Roland, F. (1996) *J. Biol. Inorg. Chem. 1*, 567−574.
15. Hoare, D. G., & Koshland, D. E. (1967) *J. Biol. Chem. 242*, 2447−2453.
16. Crichton, R. R., & Bryce, C. F. A. (1973) *Biochem. J. 131*, 289−299.
17. Gallois, B., Langlois d'Estaintot, B., Michaux, M.-A., Dautant, A., Granier, T., Précigoux, G., Soruco, J. A., Roland, F., Chavez-Alba, O., Herbas, A., & Crichton, R. R. (1997) *J. Biol. Inorg. Chem. 2*(3) (in press).
18. Michaux, M.-A. (1996) Thèse de Doctorat, Université de Bordeaux I, Bordeaux, France.

BI9709147